Inorg. Chem. **2007**, *46*, 238–250

Dinuclear Complexes Formed with the Triazacyclononane Derivative ENOTA^{4-}: High-Pressure ^{17}O NMR Evidence of an Associative Water Exchange on [Mn^{II}_2(ENOTA)(H_2O)$_2$]

Edina Balogh,[†] Zhenjie He,[‡] Wenyuan Hsieh,[‡] Shuang Liu,[‡] and Éva Tóth*[,†,§]

Laboratoire de chimie inorganique et bioinorganique, Ecole Polytechnique Fédérale de Lausanne, CH-1015 Lausanne, Switzerland, School of Health Sciences, Purdue University, West Lafayette, Indiana 47907, and Centre de Biophysique Moléculaire, CNRS, rue Charles Sadron, 45071 Orléans, France

Received September 1, 2006

Mn^{2+} has five unpaired d-electrons, a long electronic relaxation time, and labile water exchange, all of which make it an attractive candidate for contrast agent application in medical magnetic resonance imaging. In the quest for stable and nonlabile Mn^{2+} complexes, we explored a novel dimeric triazacyclononane-based ligand bearing carboxylate functional groups, H_4ENOTA. The protonation constants of the ligand and the stability constants of the complexes formed with some endogenously important metals (Ca^{2+}, Cu^{2+}, Zn^{2+}), as well as with Mn^{2+} and Ce^{3+}, have been assessed by NMR methods, potentiometry, and UV–vis spectrophotometry. Overall, the thermodynamic stability of the complexes is lower as compared to that of the corresponding NOTA analogues (H_3NOTA, 1,4,7-triaazacyclononane-1,4,7-triacetic acid). The crystal structure of Mn_2(ENOTA)(H_2O)·5H_2O contains two six-coordinated Mn^{2+}, in addition to the three amine nitrogens and the two oxygens from the pendent monodentate carboxylate groups, and one water (Mn2) or one bridging carboxylate oxygen (Mn1) completes the coordination sphere of the metal ion. In an aqueous solution, this bridging carboxylate is replaced by a water molecule, as evidenced by the ^{17}O chemical shifts and proton relaxivity data that point to monohydration for both metal ions in the dinuclear complex. A variable-temperature and -pressure ^{17}O NMR study has been performed on [Mn_2(ENOTA)(H_2O)$_2$] to assess the rate and, for the first time on a Mn^{2+} chelate, also the mechanism of the water exchange. The inner sphere water is slightly more labile in [Mn_2(ENOTA)(H_2O)$_2$] ($k_{ex}^{298} = 5.5 \times 10^7$ s^{-1}) than in the aqua ion (2.1×10^7 s^{-1}, Merbach, A. E.; et al. *Inorg. Chem.* **1980**, *19*, 3696). The water exchange proceeds via an almost limiting associative mechanism, as evidenced by the large negative activation volume ($\Delta V^{\ddagger} = -10.7$ cm^3 mol^{-1}). The proton relaxivities measured on [Mn_2(ENOTA)(H_2O)$_2$] show a low-field dispersion at ~0.1 MHz arising from a contact interaction between the Mn^{II} electron spin and the water proton nuclear spins.

Introduction

The spectacular ascension of magnetic resonance imaging (MRI) in clinical diagnostics is largely related to the successful use of contrast-enhancing agents.[1,2] Although the majority of the paramagnetic chelates used today in clinical practice are based on Gd^{3+}, there is continuous interest in developing Mn^{2+} complexes for MRI applications. Mn^{2+} has five unpaired d-electrons, a long electronic relaxation time, and labile water exchange, all of which make it an attractive candidate. Moreover, the ionic radius of Mn^{2+} is very similar to that of Ca^{2+} and, therefore, it is able to interfere in Ca^{2+} channels.[3]

The efficiency of a paramagnetic chelate as an MRI contrast agent is expressed by its proton relaxivity, the paramagnetic enhancement of the longitudinal relaxation rates of the bulk water protons, referred to 1 mM concentra-

* To whom correspondence should be addressed. Fax: +33 2 38 63 15 17. Telephone: +33 2 38 25 76 25. E-mail: eva.jakabtoth@cnrs-orleans.fr.
† Ecole Polytechnique Fédérale de Lausanne.
‡ Purdue University.
§ CNRS.

(1) Caravan, P.; Ellison, J. J.; McMurry, T. J.; Lauffer, R. B. *Chem. Rev.* **1999**, *99*, 2293.
(2) *The Chemistry of Contrast Agents in Medical Magnetic Resonance Imaging*; Tóth, É., Merbach, A.E., Eds.; John Wiley & Sons: Chichester, 2001.
(3) *NMR Biomed.* **2004**, *17* (8). Issue dedicated to manganese enhanced magnetic resonance imaging.

10.1021/ic0616582 CCC: $37.00
Published on Web 12/07/2006

tion of the agent. The paramagnetic relaxation effect originates from two distinct mechanisms: the inner sphere relaxation term is related to short-distance interactions between the paramagnetic metal ion and the water protons in the inner coordination sphere, while the outer sphere relaxation term is the result of long-distance interactions between the metal ion and water protons diffusing in the proximity of the complex. To take advantage of the inner sphere mechanism, at least one water molecule should be coordinated in the inner sphere.

MRI application would, therefore, require ligands which form stable complexes with Mn^{2+} but leave enough space in the inner coordination sphere for at least one water molecule. Today, there is only one clinically approved Mn^{2+} compound, $MnDPDP^{4-}$, which is mainly used for the detection of liver diseases or for cardiac imaging ($DPDP^{6-}$, *N*,*N*′-dipyridoxylethylenediamine-*N*,*N*′-diacetate 5,5′-bis-(phosphate)).[4] $MnDPDP^{4-}$ has no inner sphere water, and it was proved that its *in vivo* relaxation effect can be related to an important dissociation of the complex and the release of Mn^{2+} in the body. The free Mn^{2+} is then taken up by the hepatocytes.[5] The protein binding results in a distribution in the extracellular space and a consequent slow body clearance. The presence of the DPDP ligand is necessary because it induces a slower release of manganese than would have been the case had manganese been administered as a simple salt, such as manganese chloride.

Aime et al. studied one DO3A (1,4,7,10-tetraazacyclododecane-1,4,7-triacetic acid)- and two EDTA-derivative Mn^{2+} complexes bearing benzyloxymethyl (BOM) substituents, which allow for efficient protein binding.[6] In an ^{17}O NMR and nuclear magnetic relaxation dispersion (NMRD) study, they found that the macrocyclic $[Mn(DO3A)(BOM)_3]^-$ complex had no inner sphere water, while the ethylenediaminetetraacetate (EDTA) derivatives both contained one water molecule. In the presence of serum albumin, a significant enhancement of the proton relaxivity was observed for the EDTA derivatives (up to $\sim$58 mM^{-1} s^{-1} at 20 MHz). The field-dependent NMRD profiles of these systems were later reinterpreted by Kowalewski et al. using theoretical models that take into consideration a multiexponential electron spin relaxation.[7] More recently, Caravan et al. reported another EDTA-derivative Mn^{2+} complex which contains the same protein binding diphenylcyclohexyl moiety as the Gd^{3+}-based contrast agent MS-325.[8] The high relaxivity under biological conditions (46 mM^{-1} s^{-1} at 20 MHz, 37 °C in human plasma) could be rationalized in terms of an efficient exchange of the coordinated water and a slow tumbling of the system due to protein binding.

Chart 1

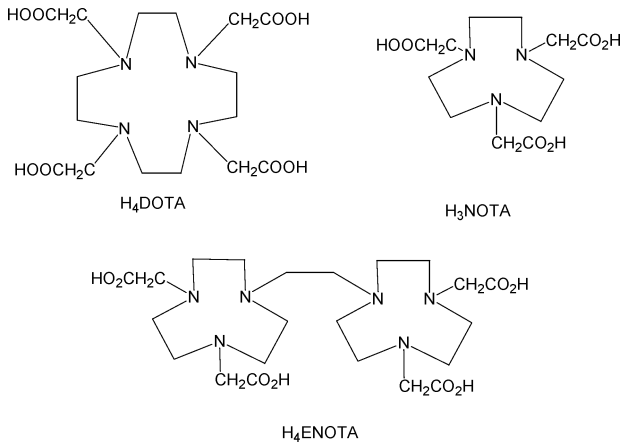

The *in vivo* toxicity of a poly(amino carboxylate) complex is mainly related to its thermodynamic stability and kinetic inertness. In general, Mn^{2+} complexes have low thermodynamic stability, originating from the lack of ligand field stabilization energy in a high-spin d^5 electronic configuration. Moreover, Mn^{2+} complexes, even with relatively high thermodynamic stability, such as $MnDTPA^{3-}$, are kinetically labile and easily release the metal ion in the body via metal exchange reactions with divalent cations, such as Ca^{2+}, Mg^{2+}, or Zn^{2+}. This leads to concerns about the potential long-term neurotoxicity associated with the use of Mn-based contrast agents. For instance, it was proved that, using linear chelators, such as $DTPA^{4-}$ or $DPDP^{6-}$, there does not exist any chelate effect protecting the brain from Mn^{2+} accumulation, since the regional distribution was the same for these complexes and the free Mn^{2+} ion.[9]

Macrocyclic metal complexes are, in general, kinetically more inert than their linear analogues. With Mn^{2+}, macrocyclic pentaamines have been investigated as superoxide dismutase catalysts and have shown increased inertness.[10] The cyclen derivatives DOTA, DO3A, HPDO3A, and 1,4- and 1,7-DO2A have also been studied, and they were proven to form thermodynamically and kinetically stable Mn^{2+} complexes (H_4DOTA, 1,4,7,10-tetraazacyclododecane-1,4,7,10-tetraacetic acid; H_3DO3A; H_3HPDO3A, 1,4,7,10-tetraazacyclododecane-1(2-hydroxypropyl)-4,7,10-triacetic acid; H_2DO2A, 1,4,7,10-tetraazacyclododecane-1,4- or 1,7-diacetic acid).[11]

In the family of triaza macrocycles, the ligand H_3NOTA (Chart 1) forms relatively stable 1:1 complexes with a number of metal ions, such as Al^{3+}, Cr^{3+}, Mn^{2+}, Mn^{3+}, Fe^{2+}, Fe^{3+}, and so forth.[12−14] In these complexes, the ligand has been found to be coordinated in a hexadentate manner. In

(4) (a) Rocklage, S. M.; Cacheris, W. P.; Quay, S. C.; Hahn, F. E.; Raymond, K. N. *Inorg. Chem.* **1989**, *28*, 477. (b) Murakami, T.; Baron, R. L.; Peterson, M. S.; Oliver, J. H., III; Davis, P. L.; Confer, B. S.; Federle, M. P. *Radiology* **1996**, *200*, 69.
(5) Ballez, B.; Bacic, G.; Swartz, H. M. *Magn. Reson. Imaging* **1996**, *35*, 14.
(6) Aime, S.; Anelli, P. L.; Botta, M.; Brochetta, M.; Canton, S.; Fedeli, F.; Gianolio, E.; Terreno, E. *JBIC, J. Biol. Inorg. Chem.* **2002**, *7*, 58.
(7) Kruk, D.; Kowalewski, J. *JBIC, J. Biol. Inorg. Chem.* **2003**, *8*, 512.
(8) Troughton, J. S.; Greenfield, M. T.; Greenwood, J. M.; Dumas, S.; Wiethoff, A. J.; Wang, J.; Spiller, M.; McMurry, T. J.; Caravan, P. *Inorg. Chem.* **2004**, *43*, 6313.
(9) Gallez, B.; Baudelet, C.; Geurts, M. *Magn. Reson. Imaging* **1998**, *16*, 1211.
(10) Riley, D. P.; Lennon, P. J.; Neumann, W. L.; Weiss, R. H. *J. Am. Chem. Soc.* **1997**, *119*, 6522.
(11) Bianchi, A.; Calabi, L.; Giorgi, C.; Losi, P.; Mariani, P.; Palano, D.; Paoli, P.; Rossi, P.; Valtancoli, B. *Dalton Trans.* **2001**, 917.
(12) Takahashi, M.; Takamoto, S. *Inorg. Chem.* **1977**, *50*, 3413.
(13) Van der Merwe, M. F.; Boeyens, F. C. A.; Hancock, R. D. *Inorg. Chem.* **1983**, *22*, 3489.
(14) Van der Merwe, M. F.; Boeyens, F. C. A.; Hancock, R. D. *Inorg. Chem.* **1985**, *24*, 1208.

Scheme 1. Synthesis of H_4ENOTA

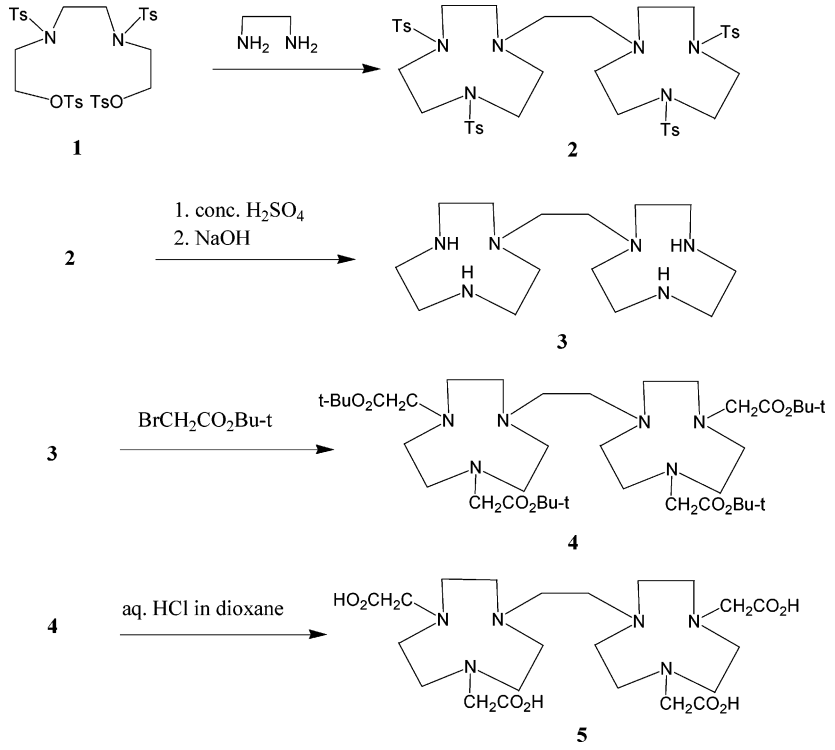

contrast to the linear analogues, such as $EDTA^{4-}$, which form much more flexible complexes, in the NOTA chelates, the metals are six-coordinate without inner sphere water molecules. This is typically the case for Mn^{2+}, which forms a monohydrated, heptacoordinate complex with EDTA,[15−17] while in the six-coordinate $MnNOTA^-$ there is no inner sphere water. This was proved by proton NMRD measurements; the relaxivities of $MnNOTA^-$ corresponded to an exclusively outer sphere contribution.[18] With regard to their thermodynamic stability, NOTA complexes are similar to the EDTA analogues, with the exception of Mg^{2+}, for which NOTA shows a significant size selectivity over Ca^{2+}.[14,19] Other triazacyclononane derivatives, in particular 1,4,7-trimethyl-1,4,7-triazacyclononane, have been largely investigated with Mn^{2+} as potent low-temperature bleaching catalysts for application in detergents.[20]

In the quest for stable Mn^{2+} complexes, here we explore a dimeric triazacyclononane-based ligand, H_4ENOTA (Chart 1). The protonation constants of the ligand and the stability constants of the complexes formed with transition metals and lanthanides have been assessed by NMR methods, potentiometry, and UV−vis spectrophotometry. The crystal structure of $Mn_2(ENOTA)(H_2O)\cdot 5H_2O$ has been determined. The dinuclear Mn^{2+} chelate has been the subject of a variable-temperature and -pressure ^{17}O NMR study, which allowed us to assess the rate and, for the first time on a Mn^{2+} chelate, also the mechanism of the water exchange. In addition, proton relaxivity measurements as a function of the magnetic field have been carried out on $[Mn_2(ENOTA)(H_2O)_2]$ to characterize its relaxation properties. The ^{17}O NMR and NMRD data have been analyzed simultaneously on $[Mn_2(ENOTA)(H_2O)_2]$, which is a general practice for potential Gd^{3+}-based contrast agents.

Experimental Section

Synthesis of H_4ENOTA (Scheme 1). The tosylate **2** was prepared as described in the literature.[21] Under a dry nitrogen atmosphere, the tosylate **2** (5.0 mmol) was added into 20 mL of concentrated sulfuric acid. The resulting mixture was heated at 100 °C with stirring for 60 h to give a brown solution and then cooled to room temperature. To another round flask charged with a stirring bar was added 150 mL of ∼20% NaOH aqueous solution containing 30 g of NaOH pellets. This flask was immersed into an ice-water bath, and the NaOH solution was vigorously stirred while the brown reaction mixture was added portionwise. After the addition was complete, the resulting mixture (pH > 12) was extracted three times with $CHCl_3$ (3 × 100 mL). The chloroform layers were combined, washed with the saturated brine (2 × 40 mL), and dried over anhydrous sodium sulfate. After filtration, the chloroform was removed under reduced pressure to give the free polyamine **3** in 100% yield as a pale yellow oil which solidifies as a white crystalline solid on standing. **3**: ^1H NMR ($CDCl_3$) δ 2.73 (s, 8H), 2.71 (m, 8H), 2.68 (s, 4H), 2.59 (m, 8H), 2.12 (br s, 4H); ^{13}C NMR ($CDCl_3$, ppm) δ 56.0, 53.3, 46.7, 46.6.

ENOTA Tetrabutyl Ester. To a stirred solution of the free polyamine (3.0 mmol) in 40 mL of anhydrous acetonitrile was added a solution of *tert*-butyl bromoacetate (13.2 mmol) in 10 mL of

(15) Richards, S.; Pedersen, B.; Silverton, J. V.; Hoard, J. L. *Inorg. Chem.* **1964**, *3*, 27.
(16) Oakes, J.; Smith, E. G. *J. Chem. Soc., Faraday Trans.* **1981**, *77*, 299.
(17) Stezowski, J. J.; Countryman, R. *Inorg. Chem.* **1973**, 12, 1749.
(18) Geraldes, C. F. G. C.; Sherry, A. D.; Brown, R. D. I.; Koenig, S. H. *Magn. Reson. Med.* **1986**, *3*, 242.
(19) Bevilacqua, A.; Gelb, R.T.; Hobard, W. B.; Zompa, L. F. *Inorg. Chem.* **1987**, *26*, 2699.
(20) Sibbons, K. F.; Shastri, K.; Watkinson, M. *Dalton Trans*. **2006**, 645 and references therein.
(21) Pulacchini, S.; Shastri, K.; Dixon, N. C.; Watkinson, M. *Synthesis* **2001**, *16*, 2381.

acetonitrile over 15−20 min under nitrogen. The resulting mixture was stirred at room temperature for 3 h. Triethylamine (18.0 mmol) was added into the reaction mixture, and the resulting mixture was stirred at room temperature another 20−21 h. The solvent and volatiles were removed on a rotary evaporator to give a white solid, which was dissolved in 20 mL of distilled water and then basified to pH > 12 by adding 20% aqueous NaOH solution followed by extraction with ether (3 × 50 mL). The ethereal layers were combined, washed with water (30 mL), and dried over sodium sulfate and filtered. Removal of the solvent gave a pale yellow solid, which was purified by column chromatography on a neutral alumina stationary phase eluted with CH_2Cl_2−methanol (20:1). The yield was 77%. Elemental analysis for $C_{38}H_{72}N_6O_8$: found (calcd) C 61.63 (61.59), H 9.47 (9.79), N 11.36 (11.34). ^{1}H NMR ($CDCl_3$, chemical shift in ppm relative to TMS): 3.30 (s, 8H), 2.85 (br s, 16H), 2.75 (br s, 8H), 2.64 (s, 4H), 1.45 (s, 36H). ^{13}C NMR ($CDCl_3$, chemical shift in ppm relative to TMS): 171.5, 80.6, 59.8, 56.9, 55.9, 55.4, 28.2.

H_4ENOTA. To a stirred solution of the tetrabutyl ester **4** (1.0 mmol) in 30 mL of dioxane was added 30 mL of 12 N HCl at room temperature. The resulting mixture was stirred for 48 h. The desired product ENOTA was formed as a white precipitate, which was collected by filtration, washed with dioxane, and dried under vacuum. The yield was nearly quantitative as its pentahydrochloride salt $C_{22}H_{40}N_6O_8$·5HCl. Elemental analysis: found (calcd) C 37.71 (37.81), H 6.39 (6.49), N 11.81 (12.02). ^{1}H NMR (D_2O): 3.78 (s, 8H), 3.35−3.20 (m, 28H). ^{13}C NMR (D_2O, ppm, using $CDCl_3$ as internal reference): 167.7, 65.6, 65.1, 59.9, 49.5.

Sample Preparation. Stock solutions of metal ions were prepared from their salts in double-distilled water. The concentrations of the solutions were determined by complexometric titration with a standardized Na_2H_2EDTA solution using xylenol orange (Zn^{2+} and Ce^{3+}) or eriochrome black-T (Ca^{2+} and Mn^{2+}) as the indicator. The concentration of the Cu^{2+} solution was determined by gravimetry. The ligand stock solution was prepared in double-distilled water; exact ligand concentrations were determined by pH−potentiometric titration. In these measurements, the difference between the two inflection points of the titration curve corresponds to 2 equiv of the ligand.

Equilibrium Measurements. The protonation constants were determined by pH−potentiometric titration at 25 °C in 0.1 M KCl except for the two highest log K_H values, which were obtained by measuring the proton NMR chemical shifts of the ligand at different pHs (between pH 10 and 14). Stability constants with Zn^{2+}, Cu^{2+}, Ca^{2+}, and Mn^{2+} were determined by pH−potentiometric titrations, at 1:1 and 1:2 L−M ratios (I = 0.1 M KCl). The samples (3 mL) were stirred, and N_2 was bubbled through the solutions. The titrations were carried out by adding a standardized KOH solution with a Metrohm Dosimat 665 automatic buret. A combined glass electrode (C14/02-SC, reference electrode Ag/AgCl in 3 M KCl, Moeller Scientific Glass Instruments, Switzerland) and a Metrohm 692 pH/ion-meter were used to measure pH. The H^+ concentration was obtained from the measured pH values using the correction method proposed by Irving et al.[22] The protonation and stability constants were calculated from several parallel titrations with the program PSEQUAD.[23] The errors given correspond to one standard deviation. The first two protonation constants of $ENOTA^{4-}$ were determined from ^{1}H NMR titration. ^{1}H NMR spectra were recorded in D_2O, and the measured pD values were converted to pH according to pD = pH + 0.4.[24]

The stability constant of the Ce^{3+} complex was determined in batch samples by UV−vis spectroscopy at 25 °C, using a thermostated cuvette holder. The ligand concentration was 1×10^{-4} M, while the metal concentration was 2×10^{-4} M. The samples were left for several days to equilibrate until no further pH change was detectable.

X-ray Crystallography of Mn_2(ENOTA)(H_2O)·5H_2O. Colorless blocks of Mn_2(ENOTA)(H_2O)·5H_2O were grown from an aqueous solution at room temperature. A crystal of dimensions 0.18 × 0.18 × 0.16 mm^3 was mounted on a standard Bruker SMART CCD-based X-ray diffractometer equipped with a normal focus Mo-target X-ray tube (λ = 0.71073 Å) operated at 2000 W power (50 kV, 40 mA). The selected crystallographic data are listed in Table S1 in the Supporting Information. The crystals were extremely sensitive to loss of water solvate and also shattered upon cooling in a low-temperature stream. Therefore, the crystal was mounted in a glass capillary with the mother liquor and the data were collected at room temperature. The cell constants and an orientation matrix for data collection were obtained from least-squares refinement, using the setting angles in the range of 2.8° < θ < 21.4°. The integration of the data yielded a total of 38 013 reflections to a maximum 2θ value of 42.78°, 5450 of which were independent and 2210 were greater than 2σ(I). The final cell constants were based on the *xyz* centroids of 5002 reflections above 10σ(I). A reference set of 50 frames was collected interspersed in the data collection to monitor for crystal decomposition. Analysis of the data showed decay during data collection on the order of 4%; the data were processed with SADABS[25] and corrected for absorption and decomposition. The structure was solved and refined with the Bruker SHELXTL (version 5.10) software package,[26] using the space group *C*2/*c* with Z = 8 for the formula $C_{22}H_{38}N_6O_8Mn_2$·6H_2O. All non-hydrogen atoms were refined anisotropically with the hydrogen atoms placed in idealized positions.

^{17}O NMR Measurements. Variable-temperature ^{17}O NMR longitudinal (T_1) and transverse (T_2) relaxation time measurements on an aqueous solution of [Mn_2(ENOTA)(H_2O)$_2$] were obtained on a Bruker ARX 400 spectrometer (9.4 T, 54.2 MHz). An acidified water solution was used as the reference ($HClO_4$, pH 3.3). In a previous work, the corresponding diamagnetic Zn^{2+} complex at identical pH and concentration values was used as the external reference.[27] However, our experience in the past showed that Zn^{2+} and acidified water references give identical results.[28] Longitudinal ^{17}O relaxation times (T_1) were measured by the inversion−recovery pulse sequence,[29] and the transverse relaxation times (T_2) were obtained by the Carr−Purcell−Meiboom−Gill spin-echo technique.[30] The samples were sealed in glass spheres fitted into 10 mm NMR tubes to eliminate susceptibility corrections to the chemical shifts.[31] The temperature was measured by a substitution technique.[32] To improve sensitivity in ^{17}O NMR, ^{17}O-enriched water

(22) Irving, H. M.; Miles, M. G.; Pettit, L. D. *Anal. Chim. Acta* **1967**, *38*, 475.
(23) Zékány, L.; Nagypál, I. *Computational Methods for Determination of Formation Constants*; Plenum Press: New York, 1985; p 291.
(24) Mikkelsen, K.; Nielsen, S. O. *J. Phys. Chem.* **1960**, *64*, 632.
(25) Sheldrick, G. M. *SADABS*: *Program for Empirical Absorbation Correction of Area Detector Data*, version 2.10; Universitiy of Gottingen: Gottingen, Germany, 2003.
(26) Sheldrick G. M. *SHELXTL*, version 5.10; Bruker Analytical X-ray: Madison, WI, 1997.
(27) Zetter, M. S.; Grant, M.; Wood, E. J.; Dodgen, H. W.; Hunt, J. P. *Inorg. Chem.* **1972**, *11*, 2701.
(28) Tóth, É. Unpublished results.
(29) Vold, R. L.; Waugh, J. S.; Klein, M. P.; Phelps, D. E. *J. Chem. Phys.* **1968**, *48*, 3831.
(30) Meiboom, S.; Gill, D. *Rev. Sci. Instrum.* **1958**, *29*, 688.
(31) Hugi, A. D.; Helm, L.; Merbach, A. E. *Helv. Chim. Acta* **1985**, *68*, 508.

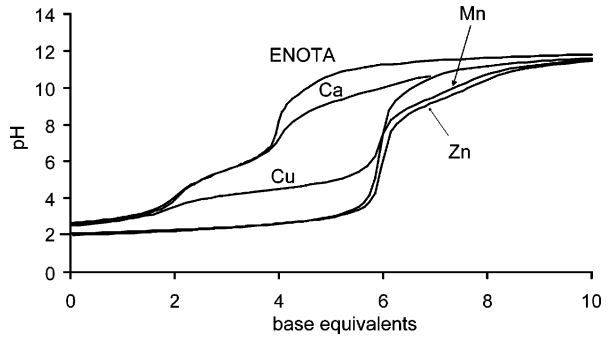

Figure 1. pH−potentiometric titration curves of H_4ENOTA solutions containing 2 equiv of HCl in the absence and in the presence of different metals at a 1:2 L−M ratio.

(11.4% $H_2{}^{17}O$, Isotrade GmbH) was added to the solutions to yield approximately 1% ^{17}O enrichment. The temperature was varied between 7.7 and 87.4 °C, c_{Mn2+} was 4.21 mmol/kg (relaxation rates) or 42.1 mmol/kg (shift measurements), and the pH was 7.4.

Variable-pressure ^{17}O relaxation rates were measured at 284 K and $c_{Mn^{2+}} = 4.26$ mmol/kg up to a pressure of 200 MPa on a Bruker ARX-400 spectrometer equipped with a homemade high-pressure probe head.[33]

NMRD. The $1/T_1$ NMRD profiles of the Mn^{2+} complex (c_{Mn} = 5 mM, pH 7.39) were recorded at 5, 25, and 37 °C with a Stelar field cycling system, covering a range of magnetic fields from 2.35 × 10^{-4} T to 0.47 T (0.01−20 MHz). Additional points were obtained on Bruker Minispec PC-20 (20 MHz), mq30 (30 MHz), mq40 (40 MHz), and mq60 (60 MHz) relaxometers.

Data Analysis. The analysis of the ^{17}O NMR and NMRD data was performed using Micromath Scientist (version 2.0; Salt Lake City, UT). The reported errors correspond to one standard deviation obtained by the statistical analysis.

Results and Discussion

Synthesis of H_4ENOTA. The ligand was prepared according to Scheme 1 by reacting 2 equiv of **1** with ethylenediamine, which produced compound **2** in its tosylate-protected form. Deprotection of the tosylate groups was achieved by dissolving **2** in concentrated sulfuric acid and heating at 100 °C for 3 days to afford the sulfate salt of **3**. The sulfate salt of **3** was neutralized by sodium hydroxide to give the corresponding free amine, which was then allowed to react with excess $BrCH_2COO^tBu$ in AcCN in the presence of triethylamine to give the *tert*-butyl ester **4**. The *tert*-butyl ester was generally obtained in high purity (>85%). If not, it could be subjected to flash column chromatography to remove the unreacted $BrCH_2COO^tBu$ and other impurities. Hydrolysis of **4** in an HCl solution of dioxane produced the final product H_4ENOTA in its pentahydrochloride salt form. The NMR (^1H and ^{13}C), mass spectral, and elemental analysis data are completely consistent with the proposed structure.

Determination of the Protonation and Stability Constants. pH−potentiometric titrations (Figure 1) represent the most generally used technique to determine protonation constants (K_i^H, eq 1):

$$K_i^H = \frac{[H_iL]}{[H_{i-1}L][H^+]} \qquad i = 1-6 \qquad (1)$$

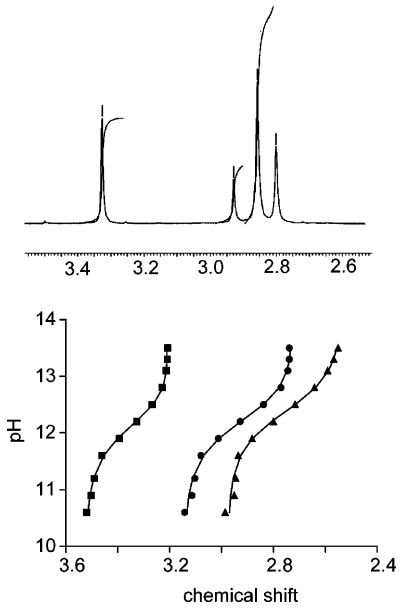

Figure 2. ^1H NMR spectrum of H_4ENOTA at pD 12.6 (top) and ^1H NMR titration curves (bottom).

Table 1. Protonation Constants of Various Macrocyclic Ligands at 25 °C and 0.1 M KCl

	$ENOTA^{4-}$	$NOTA^{3-}$ *a*	$DOTA^{4-}$ *b*
log K_{H1}	12.5(1)	11.41	12.6
log K_{H2}	12.2(1)	5.74	9.70
log K_{H3}	5.97(2)	3.16	4.50
log K_{H4}	5.18(1)	1.71	4.14
log K_{H5}	2.73(3)		2.32
log K_{H6}	1.86(3)		

[a] Reference 14. [b] Reference 34.

However, the potentiometric determination of protonation constants above pH 12 is difficult. They can be assessed by ^1H NMR spectroscopy if the chemical shifts of the nonlabile protons of the ligand exhibit a chemical shift change upon deprotonation. The first two protonation constants of $ENOTA^{4-}$ have been determined from ^1H NMR titration (Figure 2). It was necessary to add 2 equiv of base to the ligand solution to yield a pH change from 10.5 to 13.5; therefore, two protonation constants have been calculated from this region. The four subsequent protonation constants, log K_{H3-6}, have been obtained from the pH−potentiometric titration data (Figure 1) by fixing the first two constants, as calculated from ^1H NMR spectroscopy. The protonation constants obtained are given in Table 1. For comparison, the log K_i^H values of H_3NOTA and H_4DOTA are also presented.

The protonation sequence was previously determined for various cyclic polyaza polycarboxylate ligands and was found to differ considerably from that of the acyclic poly(amino carboxylates), where all the nitrogen atoms are typically protonated before the carboxylates. It has been shown that the first two protonations of the nine-membered-ring triaza tricarboxylate ligand $NOTA^{3-}$ occur on the nitrogens, while the third protonation occurs on a carboxylate.[35] The 10-

(32) Ammann, C.; Meier, P.; Merbach, A. E. *J. Magn. Reson.* **1982**, *46*, 319.
(33) Frey, U.; Helm, L.; Merbach, A. E. *High Pressure Res.* **1990**, *2*, 237.

Table 2. Stability Constants (log β), log K_{OH}, and pM Values of ENOTA and NOTA Complexes with Various Metal Ions[g]

	Zn^{2+}	Cu^{2+}	Mn^{2+}	Ca^{2+}	Ln^{3+}
		2:1 M−ENOTA ratio			
M_2L	35.88(5)	36.93(5)	24.06(5)	12.45(6)	23.3(5) (Ce)
M_2H_2L	39.85(7)		33.0(1)		
$M_2L(OH)$	−8.5(1)[a]		−9.2(1)[a]		
$M_2L(OH)_2$	−10.1(1)[a]		−10.3(1)[a]		
pM[g]	13.6	14.2	7.7	6.0	7.4
		1:1 M−ENOTA ratio			
MHL			25.2(2)		
MH_2L	36.4(1)	37.1(1)	30.2(3)		
MH_3L	37.9(2)				
		NOTA			
ML		21.63[c]	14.9[d]	8.92[c]	13.7 (Gd)[e]
MHL[b]		2.74[c]		5.06[c]	3.6[f]
pM[g]		18.6	11.8	6.2	10.6

[a] log K_{OHi} values. [b] Corresponds to K_{MHL} = [MHL]/[H][ML]. [c] Reference 19. [d] Reference 37. [e] Reference 38. [f] Reference 39. [g] pM calculated for c_{Mtotal} = 1 mM, c_{Ltotal} = 10 mM, and pH 7.4.

membered triaza macrocycle $DETA^{3-}$ has a similar protonation sequence (H_3DETA, 1,4,7-triazacyclodecane-1,4,7-triacetic acid).[36] Based on the analogy to the protonation sequence determined for $NOTA^{3-}$, the first four protonation steps of $ENOTA^{4-}$ can be attributed to two nitrogens per macrocycle, while the last two constants represent the protonation of one carboxylate in each cycle. In contrast to the case of $NOTA^{3-}$, the protonation constants for the second carboxylate of the macrocycle are below 1.8 and, thus, could not be obtained. A comparison of the protonation constants of the dimeric $ENOTA^{4-}$ to those of $NOTA^{3-}$ shows that the presence of the second cycle affects the protonation in the individual macrocycles. This is especially true for the first amine protonation, with constants being around 1 log unit higher than those in H_3NOTA. This might be related to the existence of hydrogen bonds between the amine nitrogens and the carboxylate oxygens, which is likely more important in the dimer than in the monomer. The result of such hydrogen bonding is an increased basicity for one partner (the amine, in our case) and a slightly decreased basicity for the other (the carboxylate).

The stability constants with some endogenously important metals (Zn^{2+}, Cu^{2+}, Ca^{2+}, and Mn^{2+}) have been determined by pH−potentiometric titrations, performed at 1:1 and 1:2 L−M ratios. The titration curves are shown in Figure 1, and the calculated stability constants are given in Table 2. The definition of the constants is the following:

$$xM + yH + L \rightarrow M_xH_yL \quad (2)$$

$$\beta_{M_xH_yL} = \frac{[M_xH_yL]}{[M]^x[H]^y[L]} \quad (3)$$

In the cases of Mn^{2+} and Zn^{2+}, hydroxo complexes also form in basic solutions. The constants calculated for the

(34) Burai, L.; Fabian, I.; Kiraly, R.; Szilagyi, E.; Brücher, E. *J. Chem. Soc., Dalton Trans.* **1998**, 243.
(35) Geraldes, C. F. G. C.; Alpoim, M. C.; Marques, M. P. M.; Sherry, A. D.; Singh, M. *Inorg. Chem.* **1985**, *24*, 3876.
(36) Geraldes, C. F. G. C.; Sherry, A. D.; Marques, M. P. M.; Alpoim, M. C.; Cortes, S. *J. Chem. Soc., Perkin Trans. 2* **1991**, 137.

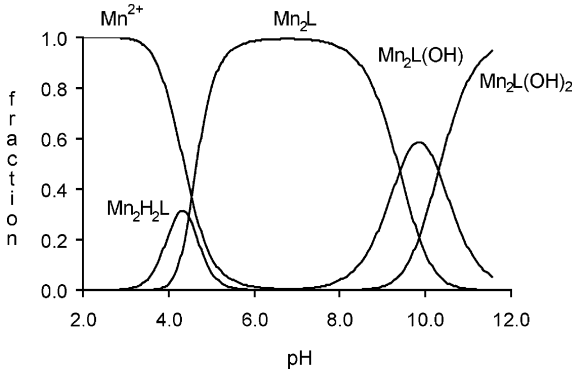

Figure 3. Species distribution curves for the Mn−ENOTA system (ENOTA = L): c_{Mn} = 0.002 M, c_{ENOTA} = 0.001 M.

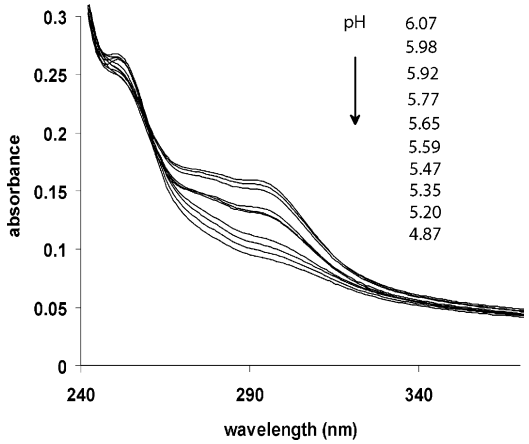

Figure 4. pH-dependent UV−vis spectra recorded in solutions of 0.0001 M ENOTA and 0.0002 M Ce^{3+}.

dissociation of the coordinated water (eqs 4 and 5) are as follows:

$$M_2L(H_2O)_n \xrightarrow{K_{OH1}} M_2L(OH)(H_2O)_{n-1} + H^+ \quad (4)$$

$$M_2L(OH)(H_2O)_{n-1} \xrightarrow{K_{OH2}} M_2L(OH)_2(H_2O)_{n-2} + H^+ \quad (5)$$

$$K_{OH1} = \frac{[M_2L(OH)(H_2O)_{n-1}][H^+]}{[M_2L(H_2O)_n]} \quad (6)$$

$$K_{OH2} = \frac{[M_2L(OH)_2(H_2O)_{n-2}][H^+]}{[M_2L(OH)(H_2O)_{n-1}]} \quad (7)$$

Potentiometric titrations have also been performed at 1:1 M−ENOTA ratios. These titration curves were analyzed by considering protonated and nonprotonated 1:1 complexes. The stability constants are presented in Table 2. It has to be noted that the comparison of the stability constants obtained at 1:1 and 1:2 ligand−metal ratios is not straightforward. It is also difficult to directly compare the stability constants for the dinuclear ENOTA and the mononuclear NOTA complexes. Therefore, we calculated pM (= −log [M_{free}]) values under conditions that are usually applied for comparing the stability of Gd^{3+} complexes in the context of MRI contrast agent applications. These pM values clearly show that that the ENOTA complexes are less stable than their

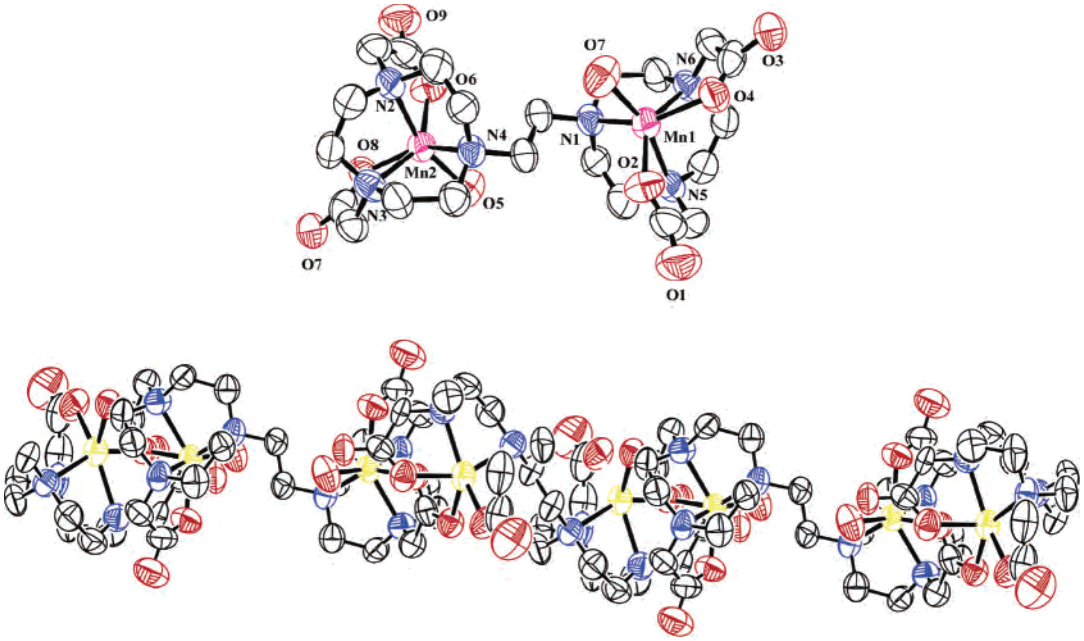

Figure 5. Top: ORTEP diagram of $Mn_2(ENOTA)(H_2O)\cdot 5H_2O$ (ellipsoids are at 50% probability). Crystallization water and hydrogen atoms are omitted for the sake of clarity. Bottom: Chain structure of the complex.

Table 3. Selected Bond Distances (Å) for $Mn_2(ENOTA)(H_2O)\cdot 5H_2O$

Mn(1)	O(2)	2.116 (8)	C(4)	O(1)	1.231 (17)
Mn(1)	O(4)	2.118 (8)	C(4)	O(2)	1.257 (17)
Mn(1)	O(7)	2.187 (7)	C(8)	O(3)	1.247 (14)
Mn(1)	N(1)	2.329 (9)	C(8)	O(4)	1.273 (14)
Mn(1)	N(5)	2.309 (10)	C(14)	O(6)	1.221 (16)
Mn(1)	N(6)	2.330 (9)	C(14)	O(9)	1.233 (19)
Mn(2)	O(5)	2.139 (8)	C(18)	O(8)	1.216 (13)
Mn(2)	O(6)	2.088 (9)	C(18)	O(7)	1.308 (13)
Mn(2)	O(8)	2.172 (8)			
Mn(2)	N(2)	2.302 (9)			
Mn(2)	N(3)	2.295 (9)			
Mn(2)	N(4)	2.282 (8)			

Table 4. Selected Bond Angles (degrees) for $Mn_2(ENOTA)(H_2O)\cdot 5H_2O$

O(2)	Mn(1)	O(4)	99.2 (3)	O(5)	Mn(2)	O(6)	95.0 (4)
O(2)	Mn(1)	O(7)	85.2 (4)	O(5)	Mn(2)	O(8)	89.1 (3)
O(4)	Mn(1)	O(7)	90.7 (3)	O(6)	Mn(2)	O(8)	92.2 (3)
O(2)	Mn(1)	N(1)	113.2 (4)	O(5)	Mn(2)	N(2)	162.4 (4)
O(4)	Mn(1)	N(1)	147.2 (4)	O(6)	Mn(2)	N(2)	75.8 (4)
O(7)	Mn(1)	N(1)	97.0 (3)	O(8)	Mn(2)	N(2)	105.9 (3)
O(2)	Mn(1)	N(5)	73.5 (4)	O(5)	Mn(2)	N(3)	117.1 (4)
O(4)	Mn(1)	N(5)	109.6 (3)	O(6)	Mn(2)	N(3)	144.2 (4)
O(7)	Mn(1)	N(5)	152.4(4)	O(8)	Mn(2)	N(3)	74.1 (3)
O(2)	Mn(1)	N(6)	144.7 (4)	O(5)	Mn(2)	N(4)	92.2 (3)
O(4)	Mn(1)	N(6)	73.5 (3)	O(6)	Mn(2)	N(4)	117.0 (3)
O(7)	Mn(1)	N(6)	128.5 (3)	O(8)	Mn(2)	N(4)	150.6 (3)
N(1)	Mn(1)	N(5)	76.3 (4)	N(2)	Mn(2)	N(3)	76.6 (4)
N(1)	Mn(1)	N(6)	76.8 (3)	N(2)	Mn(2)	N(4)	79.3 (3)
N(5)	Mn(1)	N(6)	76.7 (4)	N(3)	Mn(2)	N(4)	79.2 (3)

NOTA analogues, which is expectable on the basis of the reduced number of carboxylates. The species distribution curves are also shown for $[Mn_2(ENOTA)(H_2O)_2]$ in Figure 3.

The formation of the lanthanide complexes with H_4-ENOTA was not found to be instantaneous upon mixing of the metal and the ligand; therefore, a direct potentiometric titration could not be used to determine the stability constants. Instead, we have recorded UV−vis spectra as a function of pH for independent batch samples containing 0.0001 M ENOTA and 0.0002 M Ce^{3+}. Figure 4 shows the evolution of the spectrum in the pH range 4.8−6.1, which was used to obtain the stability constant of Ce_2ENOTA^{2+} (Table 2).

X-ray Crystallography of $Mn_2(ENOTA)(H_2O)\cdot 5H_2O$. The ORTEP drawing of $Mn_2(ENOTA)(H_2O)\cdot 5H_2O$ is shown in Figure 5; crystallization water molecules and hydrogen atoms are omitted for the sake of clarity. Selected crystallographic data are listed in the Supporting Information. Selected bond distances and bond angles are given in Tables 3 and 4, respectively. There are eight $Mn_2(ENOTA)(H_2O)\cdot 5H_2O$ molecules in each unit cell. $Mn_2(ENOTA)(H_2O)\cdot 5H_2O$ has a dimeric structure containing two six-coordinated Mn atoms. The coordination sphere of each Mn^{2+} center is occupied by three amine-N and two carboxylate-O donors from the pendent monodentate carboxylate group and a water-O donor (Mn2) or an O donor from an intermolecular bonded carboxylate (Mn1; Figure 5). The coordination geometry of the Mn^{2+} center can be described as pseudo-trigonal-prismatic. One of the trigonal planes is defined by three N atoms from the macrocyclic ring. The second trigonal plane is defined by two O atoms from the two carboxylate groups and a third O atom from either a water group (O5) or a carboxylate group from an adjacent molecule (O7). The twisted angle between two trigonal planes is 10.4°, and the angles between donor atoms that are trans to each other are in the range of 145° to 165° (Table 4). The bite angles of the N donor atoms to the Mn^{2+} center are ∼77°, and the angles of the O atom donors to the Mn^{2+} center are between 85° and 100°. The two Mn^{2+} centers are in the anti conformation with the pendent carboxylate groups from two tacn rings pointing away. These findings are consistent with those found in $[Mn_2(tmpdtne)Cl_2](ClO_4)_2\cdot 2DMF$ (average 76.0°),[40] $[Mn_2(Me_3tacn)_2(\mu\text{-}O_2CMe)_3]^+$ (average 76.5°),[41] and

(37) Cortes, S.; Brucher, E.; Geraldes, C. F. G. C.; Sherry, A. D. *Inorg. Chem*. **1990**, *29*, 5.

$[Mn(tmptacn)](ClO_4)_2$ (average 77.2°).[42] The distance between the two Mn^{2+} centers is 5.120 (3) Å, which is shorter than that found in $[Mn_2(tmpdtne)Cl_2](ClO_4)_2 \cdot 2DMF$ (6.815 (3) Å). This is due to the O atom (O7) from the carboxylate arm of the adjacent molecule being coordinated to Mn(1) intermolecularly. The average distances between Mn−O and Mn−N are 2.137 and 2.308 Å, respectively. These distances are comparable with those found in $[Mn_2(tmpdtne)Cl_2](ClO_4)_2 \cdot 2DMF$ (from the macrocycle ring Mn−N, 2.335 Å; from the pendent arm groups Mn−N, 2.237 Å) and $Cu_2(ENOTA) \cdot 5H_2O$ (Cu−O, 1.940 Å; Cu−N, 2.088 Å).[43] The adjacent $Mn_2(ENOTA)(H_2O)$ molecules are connected intermolecularly by an O atom from a carboxylate group to form an infinite chain structure with a "zigzag" shape.

^{17}O NMR and NMRD Measurements on $[Mn_2(ENOTA)(H_2O)_2]$. With regard to the inner sphere structure, $MnNOTA^-$ and $[Mn_2(ENOTA)(H_2O)_2]$ differ in their hydration state. $MnNOTA^-$ has no inner sphere water molecule, as evidenced by the low proton relaxivities originating only from outer sphere contributions. The solid-state X-ray crystallographic structure of $Mn_2(ENOTA)(H_2O) \cdot 5H_2O$ showed that, for one of the two metal ions in the dinuclear complex, one water molecule completes the inner sphere, while a bridging carboxylate coordinates to the other metal ion, leading to an overall coordination number of six for each Mn^{2+}. In an aqueous solution, this bridging carboxylate is expected to be replaced by a water molecule, which then results in an identical coordination environment involving monohydration for both metals.

In the context of MRI contrast agent applications, the paramagnetic relaxation behavior of Gd^{III} chelates is usually evaluated by ^{1}H NMRD measurements. Monitoring the proton relaxivity as a function of the magnetic field can help distinguish between various relaxation mechanisms. To get reliable information on the microscopic parameters that determine the proton relaxivity of a paramagnetic metal complex, such as the water exchange rate, rotational correlation time, and electron spin relaxation, it is advisable to complete the NMRD measurements by other techniques, which give independent access to these values. Namely, transverse ^{17}O relaxation rates allow a direct determination of the water exchange rate, while the longitudinal relaxation rates are related to the rotational motion of the complex.

We have performed a variable-temperature ^{17}O NMR study on the dinuclear $[Mn_2(ENOTA)(H_2O)_2]$ chelate, where both transverse and longitudinal relaxation rates, as well as chemical shifts, have been measured in an aqueous solution of the complex. Proton relaxivity profiles have been recorded at 25 and 37 °C up to a 60 MHz proton Larmor frequency. The ^{17}O NMR and NMRD data have been fitted together. We usually consider that such a simultaneous analysis yields more reliable and physically meaningful values for the parameters calculated, and it is routinely done for Gd^{III} chelates.

The ^{17}O NMR data have been evaluated by using the Swift and Connick equations.[44] From the measured ^{17}O NMR relaxation rates and angular frequencies of the paramagnetic solutions, $1/T_1$, $1/T_2$, and ω, and of the reference, $1/T_{1A}$, $1/T_{2A}$, and ω_A, one can calculate the reduced relaxation rates and chemical shift, $1/T_{1r}$, $1/T_{2r}$, and ω_r, which may be written as in eqs 8−10, where P_m is the molar fraction of bound water, $1/T_{1m}$ and $1/T_{2m}$ are the relaxation rates of the bound water, and $\Delta\omega_m$ is the chemical shift difference between bound and bulk water.

$$\frac{1}{T_{1r}} = \frac{1}{P_m}\left[\frac{1}{T_1} - \frac{1}{T_{1A}}\right] = \frac{1}{T_{1m} + \tau_m} \tag{8}$$

$$\frac{1}{T_{2r}} = \frac{1}{P_m}\left[\frac{1}{T_2} - \frac{1}{T_{2A}}\right] = \frac{1}{\tau_m}\frac{T_{2m}^{-2} + \tau_m^{-1}T_{2m}^{-1} + \Delta\omega_m^2}{(\tau_m^{-1} + T_{2m}^{-1})^2 + \Delta\omega_m^2} \tag{9}$$

$$\Delta\omega_r = \frac{1}{P_m}(\omega - \omega_A) = \frac{\Delta\omega_m}{(1 + \tau_M T_{2m}^{-1})^2 + \tau_m^2\Delta\omega_m^2} \tag{10}$$

$\Delta\omega_m$ is determined by the hyperfine or scalar coupling constant, $A_O/\hbar$ (eq 11), where B represents the magnetic field, S is the electron spin, and g_L is the isotropic Landé g factor.

$$\Delta\omega_m = \frac{g_L\mu_B S(S+1)B}{3k_B T}\frac{A_O}{\hbar} \tag{11}$$

The outer sphere contribution to the chemical shift was neglected.

The ^{17}O longitudinal relaxation rates are given by eq 12, where γ_S is the electron and γ_I is the nuclear gyromagnetic ratio ($\gamma_S = 1.76 \times 10^{11}$ rad s^{-1} T^{-1}, $\gamma_I = -3.626 \times 10^7$ rad s^{-1} T^{-1}), r_{MnO} is the Mn−O distance, I is the nuclear spin of ^{17}O, χ is the quadrupolar coupling constant, and η is an asymmetry parameter:

$$\frac{1}{T_{1m}} = \left[\frac{1}{15}\left(\frac{\mu_0}{4\pi}\right)^2\frac{\hbar^2\gamma_I^2\gamma_S^2}{r_{GdO}^6}S(S+1)\right]\left[6\tau_{d1} + 14\frac{\tau_{d2}}{1 + \omega_S^2\tau_{d2}^2}\right] + \frac{3\pi^2}{10}\frac{2I+3}{I^2(2I-1)}\chi^2(1 + \eta^2/3)\tau_{RO} \tag{12}$$

where

$$\frac{1}{\tau_{di}} = \frac{1}{\tau_m} + \frac{1}{\tau_{RO}} + \frac{1}{T_{ie}} \qquad i = 1,2 \tag{13}$$

τ_{RO}, the rotational correlation time, follows an exponential temperature dependence:

$$\tau_{RO} = \tau_{RO}^{298}\exp\left\{\frac{E_R}{R}\left(\frac{1}{T} - \frac{1}{298.15}\right)\right\} \tag{14}$$

(38) Brucher, E.; Cortes, S.; Chavez, F.; Sherry, A. D. *Inorg. Chem.* **1991**, *30*, 2092.
(39) Brucher, E.; Sherry, A. D. *Inorg. Chem.* **1990**, *29*, 1555.
(40) Brudenell, S. J.; Spiccia, L.; Bond, A. M.; Fallon, G. D.; Hockless, D. C. R.; Lazarev, G.; Mahon, P. J.; Tiekink, E. R. T. *Inorg. Chem.* **2000**, *39*, 881.
(41) Wieghardt, K.; Bossek, U.; Nuber, B.; Weiss, J.; Bonvoisin, J.; Corbella, M.; Vitols, S. E.; Girerd, J. J. *J. Am. Chem. Soc.* **1988**, *110*, 7398.
(42) Wieghardt, K.; Schoeffmann, E.; Nuber, B.; Weiss, J. *Inorg. Chem.* **1986**, *25*, 4877.
(43) Fly, F. H.; Graham, B.; Spiccia, L.; Hockless, D. C. R.; Tiekink, E. R. T. *J. Chem. Soc., Dalton. Trans.* **1997**, 827.

In the transverse relaxation, the scalar contribution, $1/T_{2sc}$, dominates (eq 15).

$$\frac{1}{T_{2m}} \cong \frac{1}{T_{2sc}} = \frac{S(S+1)}{3}\left(\frac{A_O}{\hbar}\right)^2\left(\tau_{s1} + \frac{\tau_{s2}}{1+\tau_{s2}^2\omega_s^2}\right) \qquad \frac{1}{\tau_{si}} = \frac{1}{\tau_m} + \frac{1}{T_{ie}} \quad (15)$$

The inverse binding time (or exchange rate, k_{ex}) of the water molecules in the inner sphere is assumed to obey the Eyring equation (eq 16), where $\Delta S^{\ddagger}$ and $\Delta H^{\ddagger}$ are the entropy and enthalpy of activation for the exchange, respectively, and k_{ex}^{298} is the exchange rate at 298.15 K.

$$\frac{1}{\tau_m} = k_{ex} = \frac{k_B T}{h}\exp\left\{\frac{\Delta S^{\ddagger}}{R} - \frac{\Delta H^{\ddagger}}{RT}\right\} = \frac{k_{ex}^{298} T}{298.15}\exp\left\{\frac{\Delta H^{\ddagger}}{R}\left(\frac{1}{298.15} - \frac{1}{T}\right)\right\} \quad (16)$$

The electronic relaxation is mainly governed by modulation of the transient zero field splitting, and for the electron spin relaxation rates, $1/T_{1e}$ and $1/T_{2e}$, McLachlan has developed the following equations:[45]

$$\left(\frac{1}{T_{1e}}\right) = \frac{32}{25}\Delta^2\left(\frac{\tau_v}{1+\omega_S^2\tau_v^2} + \frac{4\tau_v}{1+4\omega_S^2\tau_v^2}\right) \quad (17)$$

$$\left(\frac{1}{T_{2e}}\right) = \frac{32}{50}\Delta^2\left[3\tau_v + \frac{5\tau_v}{1+\omega_S^2\tau_v^2} + \frac{2\tau_v}{1+4\omega_S^2\tau_v^2}\right] \quad (18)$$

$$\tau_v = \tau_v^{298}\exp\left\{\frac{E_V}{R}\left(\frac{1}{T} - \frac{1}{298.15}\right)\right\} \quad (19)$$

where Δ^2 is the trace of the square of the transient zero-field-splitting (ZFS) tensor, τ_v is the correlation time for the modulation of the ZFS with the activation energy E_v, and ω_s is the Larmor frequency of the electron spin. In the analysis, we considered that the two Mn^{2+} centers are independent without exchange coupling. Room-temperature, solution EPR spectra obtained at X-band at 1:1 and 2:1 metal−ligand ratios showed very broad absorption bands and were practically identical. It has to be noted that several dimanganese enzymes and model compounds have been investigated[46] and showed weak antiferromagnetic exchange coupling, giving rise to complex EPR spectra that are further complicated by the effect of hyperfine coupling to ^{55}Mn.[47,48] In these systems, however, the two manganese ions are bridged by at least one glutamate or aspartate residue and often a water or hydroxide group. This is not the case in $[Mn_2(ENOTA)(H_2O)_2]$, as was shown by the X-ray structure.

The proton relaxivities (normalized to 1 mM Mn^{2+} concentration) contain both inner and outer sphere contributions:

$$r_1 = r_{1is} + r_{1os} \quad (20)$$

The inner sphere term is given by eq 21, where q is the number of inner sphere water molecules.

$$r_{1is} = \frac{1}{1000}\frac{q}{55.55}\frac{1}{T_{1m}^H + \tau_m} \quad (21)$$

The longitudinal relaxation rate of inner sphere protons, $1/T_{1m}^H$, is expressed as the sum of dipolar and scalar interactions:

$$\frac{1}{T_{1m}^H} = \frac{1}{T_1^{DD}} + \frac{1}{T_1^{SC}} \qquad i = 1 \quad (22)$$

$$\frac{1}{T_1^{DD}} = \frac{2}{15}\left(\frac{\mu_o}{4\pi}\right)^2\frac{\hbar^2\gamma_S^2\gamma_I^2}{r_{MnH}^6}S(S+1)\left[\frac{3\tau_{d1H}}{1+\omega_I^2\tau_{d1H}^2} + \frac{7\tau_{d2H}}{1+\omega_S^2\tau_{d2H}^2}\right] \quad (23)$$

$$\frac{1}{T_1^{SC}} = \frac{2S(S+1)}{3}\left(\frac{A_H}{\hbar}\right)^2\left(\frac{\tau_{e2H}}{1+\omega_s^2\tau_{e2H}^2}\right) \quad (24)$$

Here, r_{MnH} is the effective distance between the Mn^{2+} electron spin and the water protons, ω_I is the proton resonance frequency, $A_H/\hbar$ is the hyperfine or scalar coupling constant, and τ_{diH} and τ_{e2H} are given by eq 25, where τ_{RH} is the rotational correlation time of the $Mn^{2+}-H_{water}$ vector:

$$\frac{1}{\tau_{diH}} = \frac{1}{\tau_m} + \frac{1}{\tau_{RH}} + \frac{1}{T_{ie}} \qquad i = 1, 2; \qquad \frac{1}{\tau_{e2H}} = \frac{1}{\tau_m} + \frac{1}{T_{2e}} \quad (25)$$

We also consider an outer sphere contribution, described by eq 26, where N_A is the Avogadro constant and J_{os} is a spectral density function.

$$r_{1os} = \frac{32N_A\pi}{405}\left(\frac{\mu_0}{4\pi}\right)^2\frac{\hbar^2\gamma_S^2\gamma_I^2}{a_{MnH}D_{MnH}}S(S+1)[3J_{os}(\omega_I,T_{1e}) + 7J_{os}(\omega_S,T_{2e})] \quad (26)$$

$$J_{os}(\omega,T_{je}) = \mathrm{Re}\left\{\left[1 + {}^1/_4\left(i\omega\tau_{MnH} + \frac{\tau_{MnH}}{T_{je}}\right)^{1/2}\right]\Big/\left[1 + \left(i\omega\tau_{MnH} + \frac{\tau_{MnH}}{T_{je}}\right)^{1/2} + {}^4/_9\left(i\omega\tau_{MnH} + \frac{\tau_{MnH}}{T_{je}}\right) + {}^1/_9\left(i\omega\tau_{MnH} + \frac{\tau_{MnH}}{T_{je}}\right)^{3/2}\right]\right\} \qquad j = 1, 2 \quad (27)$$

For the temperature dependence of the diffusion coefficient for the diffusion of a water proton away from a Mn^{II} complex, D_{MnH}, we assume exponential temperature dependence, with activation energy E_{MnH}:

$$D_{MnH} = D_{MnH}^{298}\exp\left\{\frac{E_{MnH}}{R}\left(\frac{1}{298.15} - \frac{1}{T}\right)\right\} \quad (28)$$

(44) Swift, T. J.; Connick, R. E. *J. Chem. Phys.* **1962**, *37*, 307.
(45) McLachlan, A. D. *Proc. R. Soc. London, Ser. A* **1964**, *280*, 271.
(46) (a) Reczkowski, R. S.; Ash, D. E. *J. Am. Chem. Soc.* **1992**, *114*, 10992. (b) Khangulov, S. V.; Barynin, V. V.; Vocvodskaya, N. V.; Grebenko, A. I. *Biochim. Biophys. Acta* **1990**, *1020*, 305. (c) Antharavally, B. S.; Poyner, R. R.; Ludden, P. W. *J. Am. Chem. Soc.* **1998**, *120*, 8897.
(47) Golombek, A. P.; Hendrich, M. P. *J. Magn. Reson.* **2003**, *165*, 33.
(48) Howard, T.; Telser, J.; DeRose, V. J. *Inorg. Chem.* **2000**, *39*, 3379.

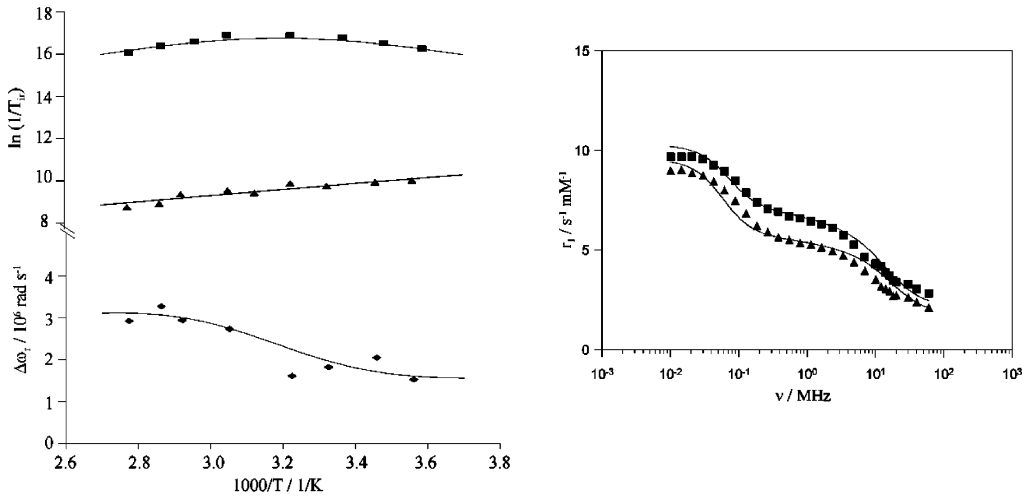

Figure 6. Left: Reduced longitudinal (▲) and transverse (■) ^{17}O relaxation rates and ^{17}O chemical shifts (♦) of $[Mn_2(ENOTA)(H_2O)_2]$ at 9.4 T. Right: ^1H NMRD profiles at 25 (■) and 37 °C (▲). The lines correspond to a simultaneous fit of all experimental data as described in the text.

Table 5. Best Fit Parameters Obtained from the Simultaneous Analysis of ^{17}O NMR and ^1H NMRD Data

parameter	$[Mn_2(ENOTA)(H_2O)_2]$	$Mn(H_2O)_6^{2+}$ [a]	$Mn(H_2O)_6^{2+}$ (308 K)[b]
$k_{ex}^{298}/10^7$ s^{-1}	5.5 ± 0.9	2.1	15
$\Delta H^{\ddagger}$/(kJ mol^{-1})	20.5 ± 1.6	32.9	
$\Delta S^{\ddagger}$/(J mol^{-1} K^{-1})	−28 ± 6	+5.7	
$\Delta V^{\ddagger}$/(cm^3 mol^{-1})	−10.7 ± 1.1	−5.4	
τ_{RO}^{298}/ps	85 ± 6		$\tau_{RH}^{308} = 30$
$A_O/\hbar$ $^{17}O/10^6$ rad s^{-1}	5.2 ± 0.6	5.3	
E_R/(kJ mol^{-1})	18 ± 1		
τ_v^{298}/ps	7.7 ± 0.6	3.3	1.5
E_v/(kJ mol^{-1})	24.8 ± 0.9	16.3	
$\Delta^2/10^{18}$ s^{-2}	4.7 ± 0.2	5.6	3.9
$A_H/\hbar$ $^1H/10^6$ rad s^{-1}	2.9 ± 0.3		4.3

[a] From ^{17}O NMR. See ref 49. [b] From the NMRD profile at a single temperature. Outer sphere contribution is neglected. See ref 50.

Altogether, a high number of parameters are involved in the simultaneous fit of the ^{17}O NMR and NMRD data, with several of them common to both data sets. The quadrupolar coupling constant for the bound water oxygen, $(\chi(1 + \eta^2)/3)^{1/2}$, was fixed to the value for pure water, $(\chi(1 + \eta^2)/3)^{1/2} = 7.58$ MHz. The Mn-coordinated water−oxygen distance was set to the value determined by the X-ray study, $r_{MnO} = 2.139$ Å, the Mn−inner sphere proton distance, r_{MnH}, was fixed to 2.75 Å, and the Mn−outer sphere proton distance, a_{MnH}, was fixed to 3.2 Å. Rotational correlation times have been calculated independently for the Mn−O and Mn−H vectors, based on the ^{17}O and ^1H T_1 data, respectively. Their ratio was obtained to be $\tau_{RH}/\tau_{RO} = 0.3 \pm 0.1$. The diffusion coefficient was fixed to $D_{MnH} = 23 \times 10^{10}$ m^2 s^{-1}, and its activation energy was fixed to $E_{MnH} = 18$ kJ mol^{-1}. The experimental data and the fitted curves are shown in Figure 6 , and all calculated parameters are given in Table 5.

To assess the mechanism of water exchange on the $[Mn_2(ENOTA)(H_2O)_2]$ complex, we have carried out variable-pressure ^{17}O transverse relaxation rate measurements at 284 K. The pressure dependence of $\ln(k_{ex})$ is given in eq 29, where $\Delta V^{\ddagger}$ is the activation volume and $(k_{ex})_0^T$ is the water exchange rate at zero pressure and temperature T.

$$\frac{1}{\tau_m} = k_{ex} = (k_{ex})_0^T \exp\left\{-\frac{\Delta V^{\ddagger}}{RT}P\right\} \qquad (29)$$

At the temperature and magnetic field used in the variable-pressure study, $1/T_{2r}$ is in the intermediate−slow exchange regime. The increase of $1/T_{2r}$ with pressure is, therefore, due to the acceleration of the water exchange process and suggests an associative (A) or associative interchange (I_a) mechanism.[51,52] The scalar coupling constant ($A/\hbar$) was previously found to be independent of pressure,[53] so we assume that it is constant and equal to the value in Table 5. τ_v was also assumed to be pressure independent. Nevertheless, we also calculated the activation volume by ascribing to τ_v a pressure dependence equivalent to activation volumes of −1 and +1 cm^3 mol^{-1} and this resulted in a change of ±1 cm^3 mol^{-1} for the fitted $\Delta V^{\ddagger}$ value. In any case, the error on $\Delta V^{\ddagger}$ is usually considered to be ±1 cm^3 mol^{-1} or 10% of the $\Delta V^{\ddagger}$ value, whichever is the largest, to take into account possible effects of nonrandom errors. The experimental data points and the results of the least-squares fit are shown in Figure 7. The fitted parameters are presented in Table 5.

Hydration Number and Water Exchange. In the analysis of the NMRD and ^{17}O NMR data, we considered that the two manganese ions coordinated in the two macrocyclic parts of the dimer are identical in terms of hydration state and water exchange. Based on the crystal structure, as discussed above, the hydration number is expected to be $q = 1$. The proton relaxivities measured in the entire field range are considerably higher than those reported for $MnNOTA^-$, $MnDOTA^{2-}$, or $MnDTPA^{3-}$, where only outer sphere effects are operative.[18] At low fields (below ~1 MHz), the relaxivities of $[Mn_2(ENOTA)(H_2O)_2]$ are even higher than those published for $[Mn(EDTA)(H_2O)]^{2-}$ with one established inner sphere water, whereas, at fields above 1 MHz, they

(49) Ducommun, Y.; Newmann, K. E.; Merbach, A. E. *Inorg. Chem.* **1980**, *19*, 3696.
(50) Bertini, I.; Briganti, F.; Xia, Z.; Luchinat, C. J. *Magn. Reson. Imaging* **1993**, *101*, 198.
(51) Lincoln, S. F.; Merbach, A. E. *Adv. Inorg. Chem.* **1995**, *42*, 1.
(52) Helm, L.; Merbach, A. E. *Chem. Rev.* **2005**, *105*, 1923.
(53) Cossy, C.; Helm, L.; Merbach, A. E. *Inorg. Chem.* **1989**, *28*, 2699.

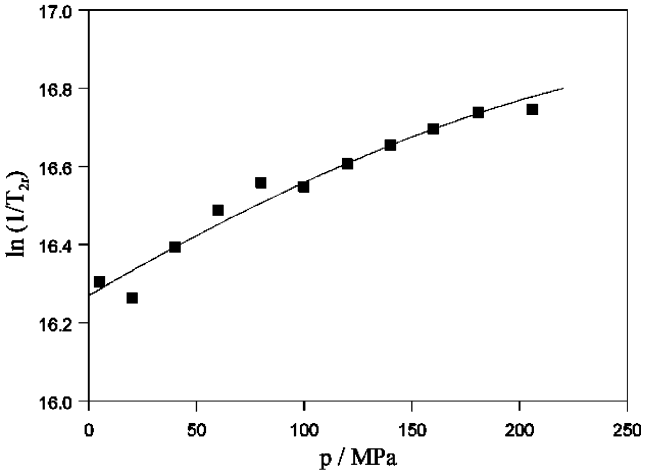

Figure 7. Variable-pressure reduced transverse ^{17}O relaxation rates measured in a $[Mn_2(ENOTA)(H_2O)_2]$ solution at 284 K and 9.4 T. The line represents a least-squares fit to the experimental data points as explained in the text.

are similar to those for $[Mn(EDTA)(H_2O)]^{2-}$. A good estimate of the number of coordinated water molecules can also be obtained from the ^{17}O NMR chemical shifts. The experimental chemical shifts are related to the value of the scalar coupling constant, and they are directly proportional to q. By assuming one inner sphere water, we obtain an $A_O/\hbar$ value which agrees well with those previously reported for various Mn^{II} chelates ($\sim$5.3 MHz). This gives us confirmation of $q = 1$.

In the past, ^{17}O NMR spectroscopy was used to assess the water exchange rate on some Mn^{II} chelates and on the $Mn(H_2O)_6^{2+}$ aqua ion itself.[49] The earliest water exchange studies involved Mn^{II}−enzyme complexes, and both increased[54] or decreased[55] labilities have been reported with respect to the aqua ion. Ligands that are less complicated than the enzymes have also been investigated (Table 6).[6,8,27,56−59] For some of the chelates, such as the 1,10-phenanthroline or the ATP compound, water exchange is only slightly accelerated upon complexation, while for others, like EDTA and EDTA derivatives, it becomes much faster. For Co^{2+} and Ni^{2+}, similar results were reported: nitrogen donors resulted in a slight acceleration of the water exchange, while oxygen donors led to an important acceleration of the water exchange.[58,60] It also has to be noted that, in some of the previous ^{17}O NMR studies on Mn^{II} complexes, the chelate was not fully formed under the conditions of the experiment due to its low stability. Therefore, both the complex and the aqua ions contributed to the experimentally measured ^{17}O relaxation rates. In that case, the determination of k_{ex} on the complex requires the separation of the two contributions, which is an additional source of inaccuracy. According to the equilibrium measurements, as shown above, the $[Mn_2(ENOTA)(H_2O)_2]$ complex is fully formed at the pH of the experiment, while the formation of the hydroxo complex is negligible (<1%). Thus, all relaxation effects measured can be attributed to the nonhydrolyzed, fully formed $[Mn_2(ENOTA)(H_2O)_2]$.

The water exchange rate is obtained from the simultaneous analysis of the ^{17}O NMR and NMRD data, but it is exclusively determined by the ^{17}O transverse relaxation rates. In the case of $[Mn_2(ENOTA)(H_2O)_2]$, the contribution of the electron spin relaxation term ($1/T_{1e}$ in τ_{s1}; eq 15) to the transverse relaxation rate varies between 5 and 50%, depending on the temperature. The small contribution of the electron spin relaxation in the fast exchange limit ensures that the value calculated for the water exchange rate is correct.

The rate of the exchange on $[Mn_2(ENOTA)(H_2O)_2]$ is 2.5 times higher than that on the aqua ion and 1 order of magnitude lower than that on $[Mn(EDTA)(H_2O)]^{2-}$. The mechanism of the exchange is associative, as evidenced by the high negative activation volume, in full accordance with the negative activation entropy. $[Mn_2(ENOTA)(H_2O)_2]$ is the first Mn^{2+} chelate for which the activation volume, and hence the mechanism, has been determined. For the seven-coordinate $[Mn(EDTA)(H_2O)]^{2-}$ and other EDTA-derivative complexes, the water exchange is expected to proceed via a dissociative mechanism. It is supported by the positive activation entropies calculated for these complexes (Table 6). Nevertheless, it has to be noted that, contrary to the activation volume, the activation entropy is not an unambiguous criterion to assess the mechanism. The very large negative value of the activation volume on $[Mn_2(ENOTA)(H_2O)_2]$ ($\Delta V^{\ddagger} = -10.7$ cm^3 mol^{-1}) points to a strong associative character of the water exchange and implies that there is largely enough space for the entrance of a second water molecule into the inner coordination sphere before the departure of the other one. Indeed, this value is approaching -13.5 cm^3 mol^{-1}, the value for a limiting associative mechanism.[50] In general terms, given the typical coordination numbers of six or seven for Mn^{2+}, one can expect that the mechanism is associative for the six-coordinate complex and dissociative for the seven-coordinate complex.

On the aqua ion $Mn(H_2O)_6^{2+}$, the water exchange proceeds via an associative interchange mechanism ($\Delta V^{\ddagger} = -5.4$ cm^3 mol^{-1}),[48] which was an unexpected result. Prior to the variable-pressure study of Merbach et al. that provided direct evidence, the mechanism was thought to be a dissociative interchange, since the complex formation rates showed low sensitivity to the nature of the entering group. The associative water exchange behavior of $Mn(H_2O)_6^{2+}$ and the gradual changeover from an associative interchange mechanism for the early octadentate, divalent transition aqua ions, such as $V(H_2O)_6^{2+}$ (ref 61) and $Mn(H_2O)_6^{2+}$, to a dissociative mechanism for the later ions, such as $Co(H_2O)_6^{2+}$ or $Ni(H_2O)_6^{2+}$, could be rationalized in terms of two factors. First, there is a significant decrease of the ionic radius along the series. The smaller the metal ion, the smaller the space left for the entering ligand to come in, and the less favorable it is for a seven-coordinate structure to be formed in the

(54) Reuben, J.; Cohn, M. *J. Biol. Chem.* **1970**, *245*, 6539.
(55) Scrutton, M. C.; Mildvan, A. S. *Biochemistry* **1968**, *7*, 1490.
(56) Gant, M.; Dodgen, H. W.; Hunt, J. P. *J. Am. Chem. Soc.* **1971**, *93*, 6828.
(57) Zetter, M. S.; Dodgen, H. W.; Hunt, J. P. *Biochemistry* **1973**, *12*, 778.
(58) Liu, G.; Dodgen, H. W.; Hunt, J. P. *Inorg. Chem.* **1977**, *16*, 2652.
(59) Grant, M.; Dodgen, H. W.; Hunt, J. P. *Inorg. Chem.* **1971**, *10*, 71.
(60) Hunt, J. P. *Coord. Chem. Rev.* **1971**, *7*, 1.
(61) Duccommun, Y.; Zbinden, D.; Merbach, A. E. *Helv. Chim. Acta* **1982**, *65*, 1385.

Table 6. Comparison of Water Exchange Parameters for Various Mn^{2+} Complexes and for the Aqua Ion[a]

parameter	CN	$k_{ex}^{298}/10^7$ s^{-1}	$\Delta H^{\ddagger}$/(kJ mol^{-1})	$\Delta S^{\ddagger}$/(J mol^{-1} K^{-1})	ref
$[Mn_2(ENOTA)(H_2O)_2]$	6	5.5 ± 0.9	20.5 ± 1.0	−28 ± 6	this work
$[Mn(phen)(H_2O)_4]^{2+}$	6	0.13 (0 °C)	43.7	+29	59
$[Mn(phen)_2(H_2O)_2]^{2+}$	6	0.31 (0 °C)	43.7	+39	59
$[Mn(ATP)(H_2O)_3]^{2-}$	7	5.0	46.3	+43	57
$[Mn(NTA)(H_2O)_2]^{-}$	6	150	32.1	+29	27
$[Mn(EDTA)(H_2O)]^{2-}$	7	44	37.4	+34	27
$[Mn(PhDTA)(H_2O)]^{2-}$	7	35	39.4	+36.9	58
$[Mn(EDTA)(BOM)(H_2O)]^{2-}$	7	9.3	43.1	+53[b]	6
$[Mn(EDTA)(BOM)_2(H_2O)]^{2-}$	7	13	38.4	+39[b]	6
$[Mn(diphen\text{-}EDTA)(H_2O)]^{2-}$	7	23	23−27		8
$Mn(H_2O)_6^{2+}$	6	2.1	32.9	+5.7	49

[a] Abbreviations: phen, 1,10-phenanthroline; ATP, adenosine-triphosphate; NTA, nitrilo-triacetate; PhDTA, *o*-phenylenediaminetetraacetate. [b] Calculated from k_{ex}^{298} and $\Delta H^{\ddagger}$.

transition state. The second, electronic factor is probably even more important: the increasing occupancy of the t_{2g} orbitals of the cation going from Mn^{2+} to Ni^{2+} also disfavors the dissociative activation mode for water exchange. The approach of the seventh molecule toward the face of the octahedron is electrostatically not favored when the t_{2g} orbitals are highly occupied; thus, a seven-coordinated state becomes less probable.

It would be of interest to see how the water exchange mechanism is affected for a series of analogous chelates formed with different-size transition metals. Unfortunately, comparisons that would also involve Mn^{2+} are not possible, not only due to the lack of experimental activation volumes, but also because the coordination mode changes with the varying cation size. This is typically the case, for example, for $EDTA^{4-}$, where the Mn^{2+} complex is seven-coordinate with one inner sphere water, while the Ni^{2+} complex is six-coordinate and shows a temperature-dependent equilibrium between a species containing hexadentate $EDTA^{4-}$ and another species with pentadentate $EDTA^{4-}$ and one water molecule.[62]

Proton Relaxivities. NMRD curves have been previously published for the Mn^{2+} aqua ion[50] and for several Mn^{II} complexes.[6,8,18] In the NMRD profiles of $[Mn_2(ENOTA)(H_2O)_2]$, one observes two dispersions, similarly to $Mn(H_2O)_6^{2+}$ and in contrast to $[Mn(EDTA)(H_2O)]^{2-}$ and EDTA derivative complexes. The low-magnetic-field dispersion at ∼0.1 MHz is known to arise from contact interaction, while the high-field dispersion at ∼10 MHz originates from the dipolar contribution.[49] The profiles of $[Mn(EDTA)(H_2O)]^{2-}$ and EDTA derivatives show only the high-field dispersion.[18] Correspondingly, the low-field relaxivities are lower (∼5−7 mM^{-1} s^{-1} at 25 °C) than those for $[Mn_2(ENOTA)(H_2O)_2]$ (∼10 mM^{-1} s^{-1}). The lack of the low-field dispersion for the EDTA-derivative complexes has been mainly attributed to a shortening of the electronic relaxation times, as compared to the case of the aqua ion,[6] which was also supported by the loss of the EPR spectrum.[16] For $[Mn_2(ENOTA)(H_2O)_2]$, we calculate T_{1e} = 5.9 ns at 20 MHz and 298 K, in contrast to the much shorter values (between 1.0 and 1.9 ns) reported for the EDTA(BOM) derivatives.[6] Another factor that certainly contributes to the appearance of the scalar contribution for $[Mn_2(ENOTA)(H_2O)_2]$ is the Mn−water proton distance, which is shorter than that in the EDTA-type chelates (2.75 Å versus 2.9 Å, based on the X-ray crystal analysis).[15] The difference in the Mn-coordinated water distance is a logical consequence of the different coordination numbers in the two types of complexes: the metal is hexacoordinated in $[Mn_2(ENOTA)(H_2O)_2]$, while it is heptacoordinated in $[Mn(EDTA)(H_2O)]^{2-}$ and EDTA derivatives.

Conclusions

We have characterized dinuclear metal complexes of a novel ligand H_4ENOTA, containing two carboxylate-functionalized triazacyclononane macrocycles. The ligand protonation constants have been determined by pH−potentiometry and ^{1}H NMR measurements, and the complex stabilities with some endogenously important metals (Ca^{2+}, Cu^{2+}, Zn^{2+}), as well as with Mn^{2+} and Ce^{3+}, have been assessed by various experimental techniques. Overall, we have found lower stabilities as compared to those of the corresponding NOTA complexes.

In the solid state, $Mn_2(ENOTA)(H_2O)\cdot 5H_2O$ has a dimeric structure containing two six-coordinated Mn atoms. The coordination sphere of each Mn^{2+} center is occupied by three amine-N donors, two carboxylate-O donors from the pendent monodentate carboxylate group, and a water-O donor (Mn2) or an O donor from an intermolecular bonded carboxylate (Mn1). In an aqueous solution, this neighboring carboxylate oxygen is replaced by a water molecule, as evidenced by the ^{17}O chemical shifts and the proton relaxivity data that point to monohydration for both metal ions in the dinuclear complex. $[Mn_2(ENOTA)(H_2O)_2]$ has been the subject of variable-temperature and -pressure ^{17}O NMR and H NMRD studies, and the data obtained by the two techniques have been analyzed together. We have found that the inner sphere water is more labile in $[Mn_2(ENOTA)(H_2O)_2]$ compared to the aqua ion. The water exchange proceeds via an almost-limiting associative mechanism, as evidenced by the large negative activation volume. This finding is in line with the associative character of the water exchange previously assessed on the six-coordinate $Mn(H_2O)_6^{2+}$ aqua ion.

Acknowledgment. We are grateful to André E. Merbach and Lothar Helm for discussions and to Meriem Benmelouka for recording the EPR spectra. We thank the Swiss National

(62) Grant, M. W.; Dodgen, H. W.; Hunt, J. P. *Chem. Commun.* **1970**, 1446.

Science Foundation and the Swiss State Secretariat for Education and Research (SER) for financial support. Acknowledgment is also made to Bristol-Myers Squibb Medical Imaging for the partial support of this research. This work was performed in the frame of the EU COST Action D18 "Lanthanide Chemistry for Diagnosis and Theraphy" and the European-founded EMIL program (LSCH-2004-503569).

Supporting Information Available: Selected crystallographic data for $Mn_2(ENOTA)(H_2O)\cdot 5H_2O$. Variable-temperature transverse and longitudinal ^{17}O relaxation rates and chemical shifts, variable-pressure transverse ^{17}O relaxation rates, and proton relaxivities for $[Mn_2(ENOTA)(H_2O)_2]$. This material is available free of charge via the Internet at http://pubs.acs.org.

IC0616582